Detecting and tracking nosocomial methicillin-resistant *Staphylococcus aureus* using a microfluidic SERS biosensor

SUPPLEMENTARY INFORMATION

Chemicals and reagents. Silver nitrate, sodium citrate, sodium chloride and mineral oil were of analytical grade and purchased from Sigma-Aldrich. The channel mold was fabricated from SU-8 3050 (MicroChem) using photolithography techniques and bonded to a glass slide substrate (12-550C, Fisher Scientific). An elastomer base and the curing agent were mixed at the mass ratio of 10:1 (Sylgard 184 silicone elastomer kit (Dow Corning)) to form polydimethylsiloxane (PDMS). Dow Corning Silastic laboratory tubing (11-189-15 Series, Fisher Scientific) was used to define inlets/outlets.

Bacterial sample collection and preparation. Two different bacterial isolate collections were used in the current study. Collection I was obtained from Tianjin Medical University General Hospital and Tianjin University, Tianjin, China, and included 38 *S. aureus* isolates collected from 2006-2011 in this hospital (Table S1a). All the isolates were recovered from inpatients and analyzed using PCR at Tianjin University of Science and Technology. Collection II was obtained from University of Washington, USA, and contained 20 *S. aureus* isolates (Table S1b). These isolates were typed by using PCR and MLST at Washington State University. All the isolates were stored frozen (-80°C) in Luria-Bertani (LB) broth containing 12% glycerol. The bacterial isolates were cultured on LB agar plates at 37°C under aerobic conditions during the course of the experiment.

Overnight cultures of *S. aureus* were harvested by centrifugation at 8,000 ×*g* to remove broth components and bacterial metabolites and the pellets were rinsed two times with phosphate buffer

saline. The cell number of resultant bacterial culture was determined and correlated to OD_{540} value. The OD_{540} value of 0.8 correlates with an averaged cell number of 4×10^8 cells per ml.

DNA extraction. DNA was extracted from the *S. aureus* isolates using the DNeasy Blood & Tissue Kit (Qiagen, Valencia, CA), following the Gram-positive extraction procedure according to manufacture protocol. DNA purity and concentration was determined by 260/280 absorbance using a NanoDrop 1000 instrument (Thermo, Brookfield, WI).

Detection of *mecA* by PCR. PCR amplification of the *mecA* gene for all the *S. aureus* isolates obtained from China was accomplished with sequence designing of specific primers as follows, F3: TGATGCTAAAGTTCAAAAGAGT, and B3: GTAATCTGGAACTTGTTGAGC. PCR amplification of the *mecA* gene for all the *S. aureus* isolates obtained from the United States was accomplished with the specific primers under the conditions described previously [1] using the specific primers MR1: GTGGAATTGGCCAATACAGG and MR2: TGAGTTCTGCAGTACCGGAT. PCR was performed using a MJ Research thermocycler (Biodirect Inc. Taunton, MA) with an initial denaturing step of 5 min at 95°C, followed by 30 cycles of 55°C for 1 min, 72°C for 1 min, and 95°C for 1 min, and a final extension for 5 min at 72°C. The PCR products were electrophoretically detected on agarose gel.

MLST. MLST was performed as described previously under the conditions and with the primer sets of Enright *et al.* [2]. A detailed analysis of the sequence types for *S. aureus* isolates is summarized in Table S2. Briefly, the seven house-keeping genes, *arcC*, *aroE*, *glp*, *gmk*, *pta*, *tpi,* and *yqiL* were PCR amplified using cycling parameters as described above. Each locus was sequenced, and aligned using the SeqMan software package (DNASTAR, Inc., Madison, WI). Sequences of each locus were trimmed according to the web-based MLST program www.mlst.net. All loci were assigned a locus

type number, followed by sequence type assignment based on loci types. Three *S. aureus* isolates did not align to any current sequence type available through the MLST web-based program. We have designated these as New ST-1, New ST-2, and New ST-3.

Microfluidic chip fabrication. The fabrication process is shown in Fig. S1. It began with deposition of a 40 μm layer of SU-8 3050 on a glass substrate (Fig. S1a). After UV exposure with masking (Fig. S1b) and SU-8 development (Fig. S1c), the SU-8 mold was defined with the desired microchannel design. To achieve precise interconnecting interface, silastic tubing was used to form inlets and outlets [3]. Tubing with knots at both ends was first aligned with the channel mold and was then fixed using a small amount of PDMS (Fig. S1d). After this tube-fixation step, more PDMS was poured onto the mold and kept at 50°C for 3 h on a hot plate for curing (Fig. S1e). The cured PDMS was carefully peeled from the SU-8 master mold (Fig. S1f) and holes were punched to connect tubing sections to the channels (Fig. S1g). The molded PDMS and two clean glass slides were treated under oxygen plasma at 50 W and 200 mT for 30 s, and then were quickly pressed together to form a sandwiched structure (Fig. S1h). Although the irreversible bonding started immediately after these pieces were brought into contact, as a last step, we chose to heat the glass/PDMS structure on a hotplate at 75°C for 5 min to strengthen the bond.

Spectral processing. We first employed a polynomial background fit [4] coupled with baseline subtraction using minima identification and discrimination via adaptive and least-squares thresholding [5] to remove fluorescence background derived from the bacterial sample, Gaussian noise, CCD background noise and cosmic noise. A spectral smooth using a 7-point Savitzky-Golay algorithm was conducted, followed by normalization for all the spectra. Normalization effectively removes spectral fluctuation derived from the small focal volume of the bacterial cells [4].

Discriminatory power. The numerical index of discrimination was calculated using Simpson's index of diversity to determine the discriminatory powers of optofluidic-based SERS typing [4].

Chemometric analysis. Before chemometric analysis, spectral reproducibility was determined by calculating the differentiation index (D_{y1y2}) value [6]. A supervised discriminant function analysis (DFA) based dendrogram model was established and validated to differentiate between MRSA and MSSA isolates from both China and the United States. The sensitivity and specificity values were calculated using Wards cluster algorithm at the cut-off value established at 99% similarity for the DFA model. A receiver operating characteristic (ROC) curve was generated, with the true positive rate (sensitivity) plotted in function of the false positive rate (1-specificity) for different cut-off points of a parameter. The AUC was subsequently calculated [7,8].

An unsupervised hierarchical cluster analysis (HCA) based dendrogram was established to determine the correlation between optofluidic-based SERS typing and MLST for epidemiology and dissemination of MRSA isolates from the United States. Bayesian probability was conducted to validate the principal components (PCs) selected by principal component analysis (PCA) for the DFA and HCA based dendrogram models and Monte Carlo estimation was subsequently performed to determine the stability of these chemometric models [4].

The cross-validated DFA-based dendrogram model was tested for the recognition rate of 20 *S. aureus* isolates derived from a recent outbreak in the summer of 2012 in a hospital in China (the second hospital affiliated with Tianjin Medical University). The prediction of these isolates was conducted by projecting the corresponding optofluidic-based SERS spectra into each PC model and the residual distances were calculated to determine the class to which the prediction data belong. Both PCR and optofluidic-based SERS typing were conducted at Tianjin University of Science and

Technology.

MRSA S-93 and MSSA S-N7 isolates were mixed forming a gradient concentration of MRSA ranging from 5% to 100% on the basis of biomass. The optofluidic-based SERS spectra were collected for each bacterial mixture and a supervised partial least squares regression (PLSR) model was established and leave-one-out cross-validated by removing one standard from the data set at a time and calibrating the remaining standards [4, 9]. This linear regression model was evaluated on the basis of several parameters including regression coefficient (R), latent variable, residual prediction deviation (RPD), and root mean square error (RMSE) of calibration and prediction [6].

References

1. Tokue, Y.; Shoji, S.; Satoh, K.; Watanabe, A.; Motomiya, M. *Antimicrob. Agents Chemother.* **1992,** *36*, 6-9.
2. Enright, M. C.; Day, N. P.; Davies, C. E.; Peacock, S. J.; Spratt, B. G. *J. Clin. Microbiol.* **2000,** *38*, 1008-1015.
3. Li, P.; Xue, W.; Xu, J. *Lab Chip Chips and Tips* **2011**.
4. Lu, X.; Huang, Q.; Miller, W. G.; Aston, D. E.; Xu, J.; Xue, F.; Zhang, H. W.; Rasco, B. A.; Wang, S.; Konkel, M.E. *J. Clin. Microbiol.* **2012,** *50*, 2932-2946.
5. Weakley, A. T.; Griffiths, P. R.; Aston, D. E. *Appl. Spectrosc.* **2012,** *66*, 519-529.
6. Lu, X.; Rasco, B. A.; Kang, D. H.; Jabal, J. M.; Aston, D. E.; Konkel, M. E. *Anal. Chem.* **2011,** *83*, 4137-4146.
7. Duraipandian, S.; Zheng, W.; Ng, J.; Low, J. J. H.; Ilancheran, A.; Huang, Z. *Anal. Chem.* **2012**, *84*, 5913-5919.
8. Lui, H.; Zhao, J.; McLean, D.; Zeng, H. *Cancer Res.* **2012**, *72*, 2491-2500.
9. Ellis, D. I.; Brewster, V. L.; Dunn, W. B.; Allwood, J. W.; Golovanov, A. P.; Goodacre, R. *Chem. Soc. Rev.* **2012,** *41*, 5706-5727.

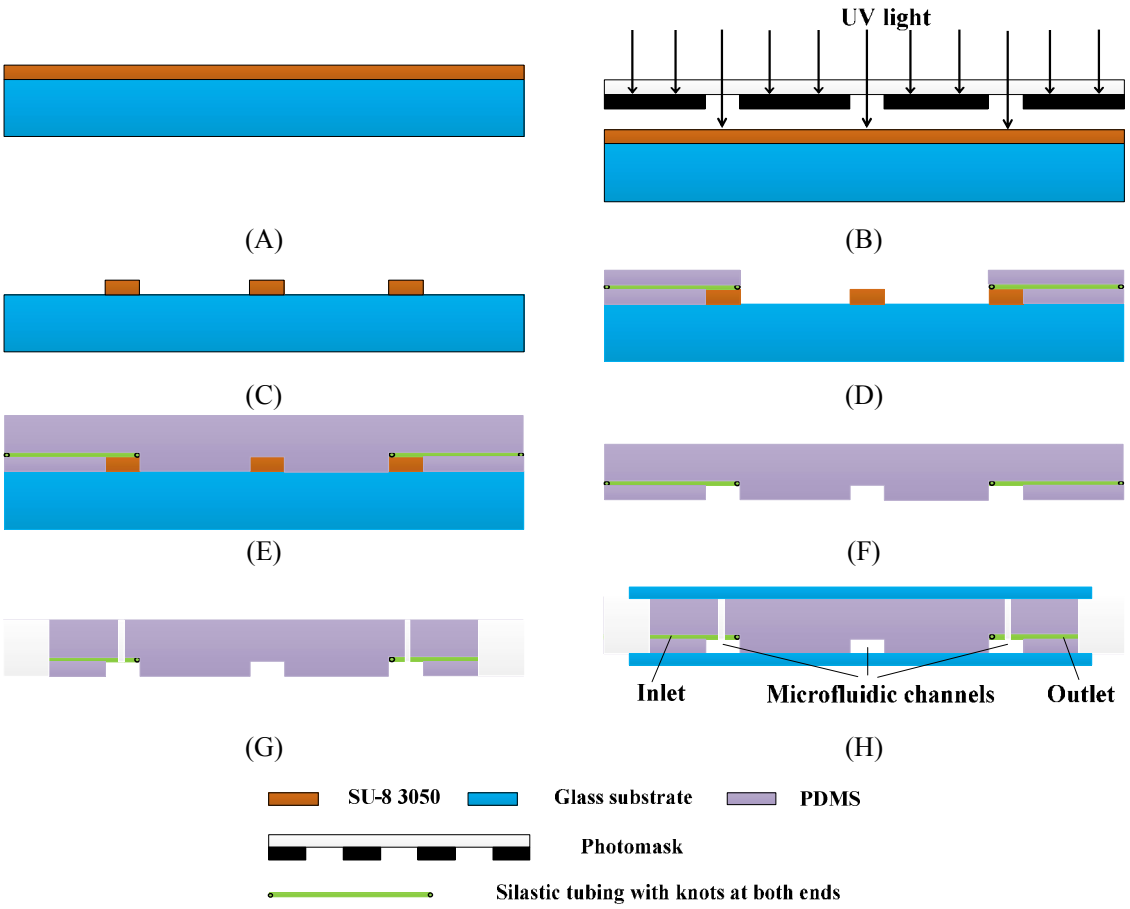

Figure S1. Fabrication process for the microfluidics channel device. (A) SU-8 spin coating on a glass substrate. (B) UV exposure with masking. (C) SU-8 development to form channel molds. (D) Alignment of tubing with the channel mold and fixation of the tubing with a small amount of PDMS. (E) Pouring more PDMS to form channels. (F) Peeling the cured PDMS. (G) Cutting the PDMS into desired size and punching holes to form inlets and outlets. (H) Bonding the PDMS to two clean glass slides.

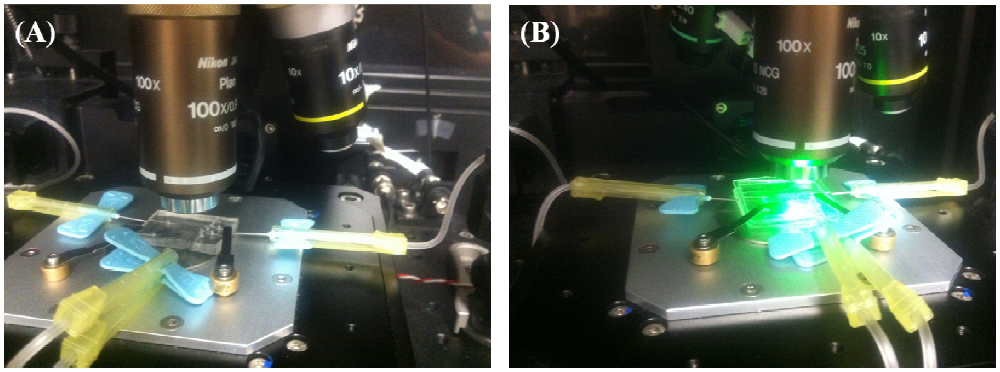

Figure S2(a). Optofluidic platform (A) without and (B) with SERS spectral collection.

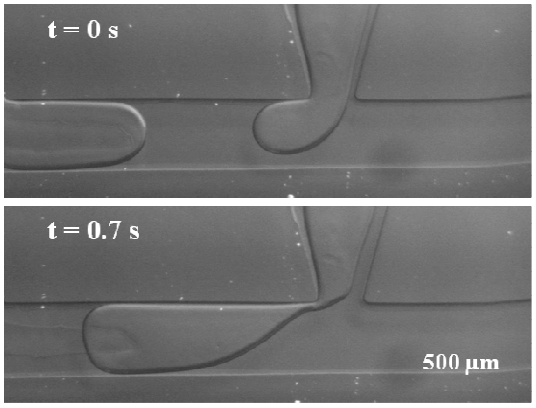

Figure S2(b). Droplet formation from the inlet of the microchannel.

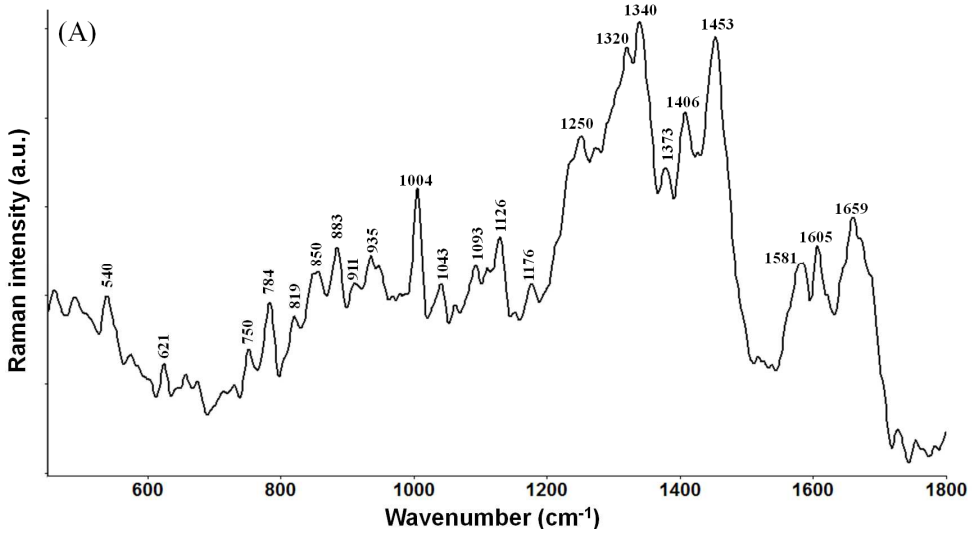

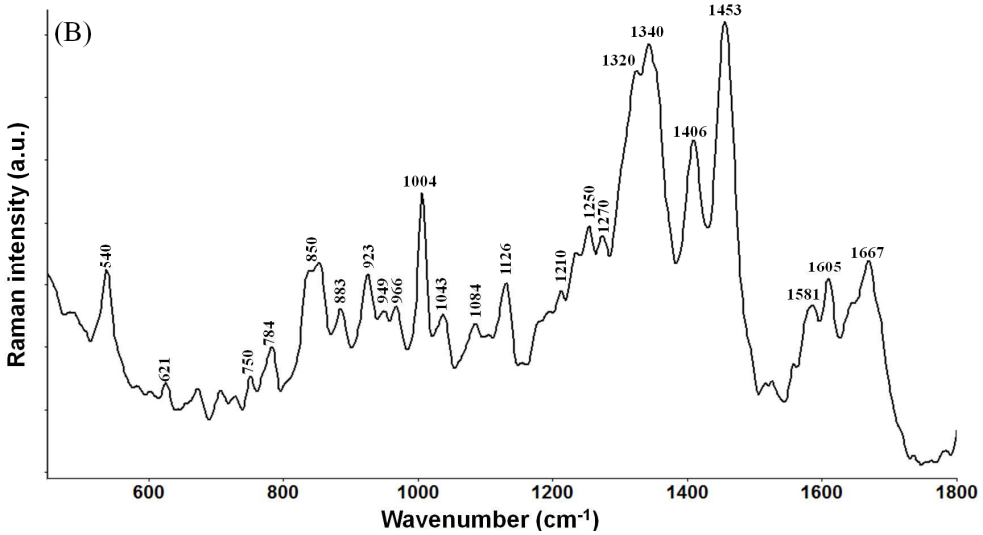

Figure S3. Biochemical compositions of *S. aureus* cell membrane: representative processed SERS spectra of (A) MRSA and (B) MSSA.

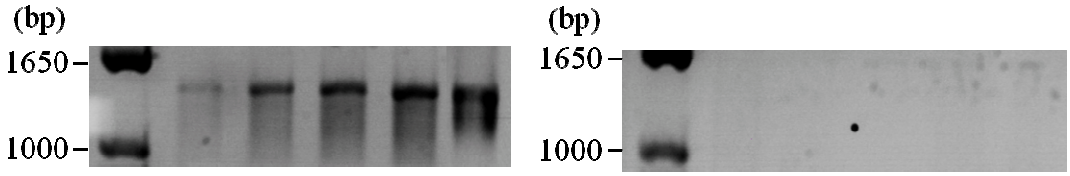

Figure S4. PCR detection of the *mecA* gene in representative *S. aureus* isolates. Panels A): MRSA; B): MSSA.

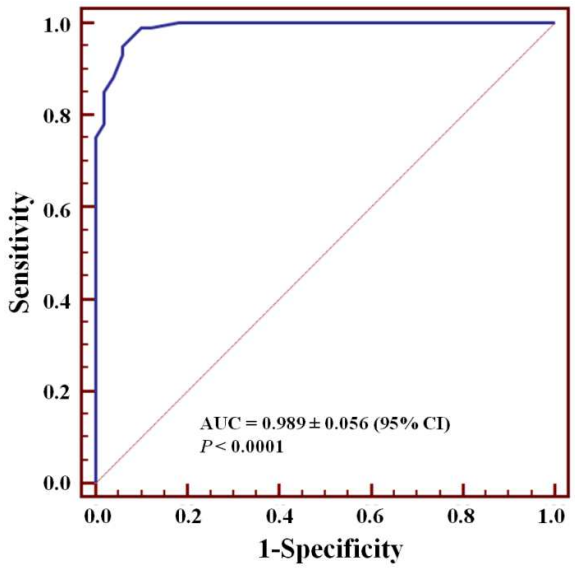

Figure S5. Receiver operating characteristic (ROC) curve of discrimination results for optofluidic SERS typing of MRSA and MSSA. The curve and 95% CI are derived from the respective cut-off thresholds and the AUC is significant ($P < 0.0001$).

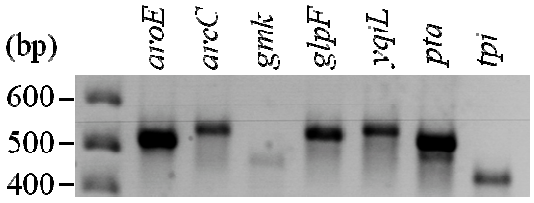

Figure S6. The allelic profile of *S. aureus* isolates.

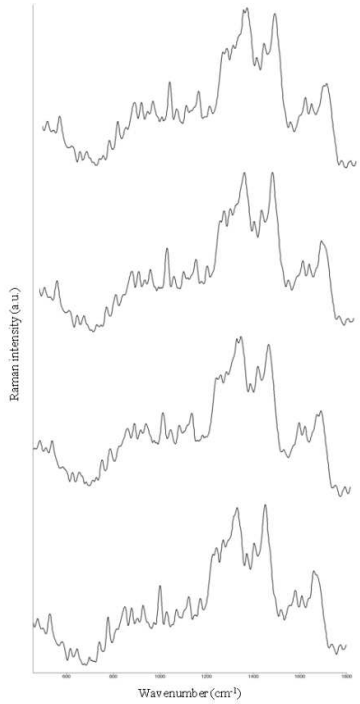

Figure S7. Optofluidic SERS spectral features of four different patterns of MRSA (from top to bottom: S-FF3 for Raman pattern 1, S-FF7 for Raman pattern 2, S-FF1 for Raman pattern 3, and S-FF9 for Raman pattern 4).

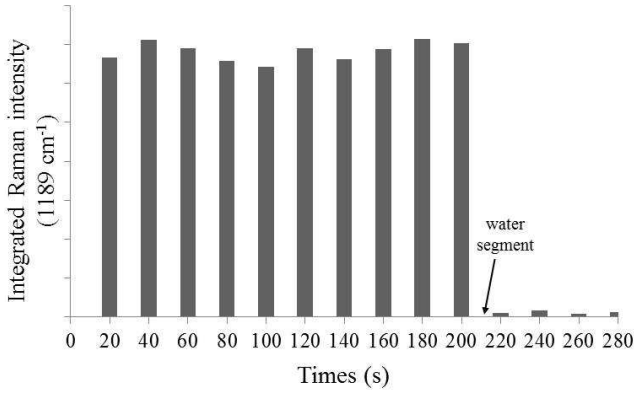

Figure S8. The SERS spectrum cannot be detected for the water segment after abrupt ceasing the flow of cystal violet.

Table S1(a). The detection of the *mecA* gene in 38 *S. aureus* isolates from China.

ID	Strain number	*mecA**	ID	Strain number	*mecA*
1	S-N4	+	20	S-93	+
2	S-N7	-	21	S-94	+
3	S-0	+	22	S-95	-
4	S-7	+	23	S-96	-
5	S-71	+	24	S-100	-
6	S-72	-	25	S-101	+

7	S-73	-	26	S-102	+
8	S-75	-	27	S-103	+
9	S-76	-	28	S-104	-
10	S-77	-	29	S-105	+
11	S-78	-	30	S-106	+
12	S-79	+	31	S-8024	+
13	S-80	-	32	S-8023	+
14	S-82	-	33	S-8021	+
15	S-83	-	34	S-5084	+
16	S-84	+	35	S-7003	+
17	S-85	+	36	S-3550	-
18	S-87	+	37	S-2821	-
19	S-89	+	38	S-2824	+

153 *The (+) indicates *mecA* positive and (-) indicates *mecA* negative.

154

155 **Table S1(b).** The detection of the *mecA* gene in 20 *S. aureus* isolates from the United States.

ID	Strain number	*mecA*	ID	Strain number	*mecA*
1	S-FF1	+	11	S-FF11	+
2	S-FF2	+	12	S-FF12	+
3	S-FF3	+	13	S-FF13	+
4	S-FF4	+	14	S-FF14	+
5	S-FF5	+	15	S-FF15	+
6	S-FF6	+	16	S-FF16	-
7	S-FF7	+	17	S-FF17	-
8	S-FF8	+	18	S-FF18	-
9	S-FF9	+	19	S-FF19	-
10	S-FF10	+	20	S-FF20	-

156

157 **Table S2.** Sequence types for *S. aureus* isolates from the United States.

S. aureus isolate	*arcC*	*aroE*	*glpF*	*gmk*	*pta*	*tpi*	*yqil*	ST
S-FF1	3	99% similar (3)*	1	1	4	4	3	New ST-1
S-FF2	3	3	1	1	4	4	3	8
S-FF3	1	145	1	19	12	1	10	New ST-2
S-FF4	3	3	1	1	4	4	3	8
S-FF5	3	3	1	1	4	4	3	8
S-FF6	3	3	1	1	4	4	3	8
S-FF7	1	4	1	4	12	1	10	5
S-FF8	3	3	1	1	4	4	3	8
S-FF9	3	3	1	1	4	4	3	8
S-FF10	3	3	1	1	4	4	3	8
S-FF11	3	3	1	1	4	4	3	8
S-FF12	3	3	1	1	4	4	3	8
S-FF13	3	3	1	1	4	4	3	8
S-FF14	3	3	1	1	4	4	3	8

S-FF15	3	3	1	1	4	4	3	8
S-FF16	2	2	2	2	6	3	2	30
S-FF17	12	31	1	4	12	1	3	New ST-3
S-FF18	3	3	1	1	4	4	3	8
S-FF19	2	2	2	2	6	3	2	30
S-FF20	1	31	1	4	12	1	10	641

158 * 99% similar to *aroE* sequence type 3: amino acid T379C

Table S3. Band assignments for the processed SERS spectra of MRSA and MSSA.

MRSA		MSSA	
Wavenumber (cm^{-1})	Band assignment	Wavenumber (cm^{-1})	Band assignment
		1667	α-helix of amide I
1659*	α-helix of amide I		
1605	phenylalanine, tyrosine, C=C (protein)	1605	phenylalanine, tyrosine, C=C (protein)
1581	phenylalanine	1581	phenylalanine
1453	C-H bending of protein	1453	C-H bending of protein
1406	ν_s COO^- of protein	1406	ν_s COO^- of protein
1373	ring breathing modes of the DNA/RNA bases		
1340	nucleic acid modes	1340	nucleic acid modes
1320	G (DNA/RNA)	1320	G (DNA/RNA)
		1270	amide III
1250	amide III	1250	amide III
		1210	C-H bending of tyrosine
1176	C-H bending of tyrosine		
1126	ν(C-C) skeletal of acyl backbone in lipid	1126	ν(C-C) skeletal of acyl backbone in lipid
1093	DNA backbone-phosphate backbone		
		1084	phosphodiester groups in nucleic acid
1043	carbohydrate	1043	carbohydrate
1004	phenylalanine	1004	phenylalanine
		966	lipids
		949	amino acids
935	α-helix of protein		
		923	C-C stretch of carbohydrate
911	C-C stretch of carbohydrate		
883	protein	883	protein
850	tyrosine	850	tyrosine
819	protein band		
784	phosphodiester	784	phosphodiester
750	symmetric breathing of tryptophan	750	symmetric breathing of tryptophan
621	C-C twisting mode of phenylalanine	621	C-C twisting mode of phenylalanine
540	ν(S-S) amino acid cysteine	540	ν(S-S) amino acid cysteine

*The numbers underlined indicate spectral bands at different wavenumbers between MRSA and MSSA.

Table S4. Recognition rate for optofluidic-based SERS spectra of *S. aureus* clinical isolates from a recent nosocomial outbreak in China.

Isolate	*mecA*	Total no. of spectra	No. of isolate spectra incorrectly classified	% of isolate spectra correctly classified
TMU2012S-1	+	100	2	98
TMU2012S-2	+	100	1	99
TMU2012S-3	-	100	8	92
TMU2012S-4	-	100	1	99
TMU2012S-5	-	100	7	93
TMU2012S-6	+	100	4	96
TMU2012S-7	+	100	0	100
TMU2012S-8	-	100	6	94
TMU2012S-9	+	100	8	92
TMU2012S-10	+	100	9	91
TMU2012S-11	+	100	5	95
TMU2012S-12	-	100	5	95
TMU2012S-13	+	100	0	100
TMU2012S-14	-	100	5	95
TMU2012S-15	-	100	5	95
TMU2012S-16	+	100	9	91
TMU2012S-17	+	100	7	93
TMU2012S-18	+	100	4	96
TMU2012S-19	+	100	5	95
TMU2012S-20	-	100	9	91
Average recognition rate (%)				95

Table S5. PLSR models for prediction of MRSA in a mixture of MSSA and MRSA.

				Calibration			Cross-validation		
Species	Conc. range (%)	No. of samples	No. of latent variables	R	RMSE [a]	RPD [b]	R	RMSE	RPD
MRSA	5-100	3300	6	≥0.99	≤0.37	≥16.19	≥0.98	≤0.44	≥10.05

[a] RMSE, root mean square error; [b] residue prediction deviation.